

International Conference on Space Optics—ICSO 2014

La Caleta, Tenerife, Canary Islands

7–10 October 2014

Edited by Zoran Sodnik, Bruno Cugny, and Nikos Karafolas



New approaches in optical rotation sensing

S. Schwartz

G. Feugnet

B. Morbieu

N. El Badaoui

et al.



International Conference on Space Optics — ICSO 2014, edited by Zoran Sodnik, Nikos Karafolas,
Bruno Cugny, Proc. of SPIE Vol. 10563, 105633Y · © 2014 ESA and CNES
CCC code: 0277-786X/17/\$18 · doi: 10.1117/12.2304190

NEW APPROACHES IN OPTICAL ROTATION SENSING

S. Schwartz¹, G. Feugnet¹, B. Morbieu², N. El Badaoui², G. Humbert³, F. Benabid³, I. Fsaifes⁴, F. Bretenaker⁴

¹ *Thales Research and Technology, Campus Polytechnique, 91767 Palaiseau Cedex, France;*

² *Thales Avionics, 40 rue de la Brelandière, BP 128, 86101 Châtellerault, France;*

³ *GPPMM Group, Xlim Research Institute, CNRS UMR 7252, University of Limoges, France;*

⁴ *Laboratoire Aimé Cotton, CNRS-Université Paris Sud 11, 91405 Orsay Cedex, France.*

INTRODUCTION

Over the last few years, there has been an increasing demand for medium-grade gyroscopes to fill the gap (in terms of cost and performance) between MEMS and current optical devices. There has also been a long-standing quest for a compact high-grade gyroscope to reduce the size of current inertial navigation units and make them available for most carriers (extending their time of GPS-free autonomous navigation).

In this paper, we will describe two approaches we are following towards these goals, with support from the European Space Agency: the solid-state ring laser gyroscope and the resonant hollow-core fiber optic gyroscope.

THE SOLID-STATE RING LASER GYROSCOPE

The first approach is the solid-state ring laser gyroscope. The basic principle is to use a solid-state (typically diode-pumped Nd-YAG) gain medium rather than the usual Helium-Neon mixture to make a ring laser gyroscope with improved lifetime, reliability and cost efficiency. In such a device, mode competition can hinder bidirectional emission and an additional stabilizing device has to be implemented. This has been achieved in our case with a feedback loop taking as the error signal the intensity difference between the two counter-propagating beams, and counter-acting on the differential losses inside the cavity. The latter are generated by changing the polarization states of the counter-propagating modes, using a combination of reciprocal rotation (thanks to a slight non-planarity of the cavity), nonreciprocal rotation (Faraday Effect within the Nd-YAG rod placed inside a solenoid) and polarizing effect (appropriate coating on one of the mirrors). The overall device is sketched on figure 1.

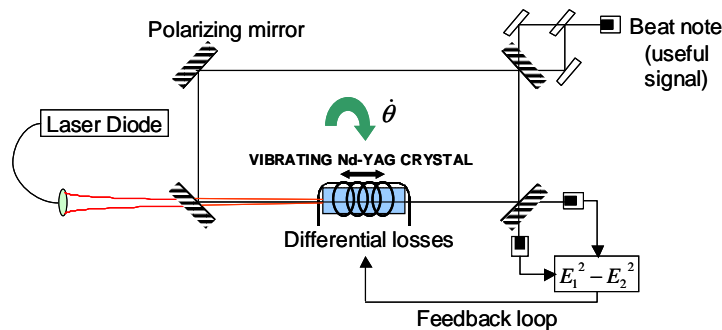


Figure 1. Sketch of our basic experimental setup.

Thanks to this stabilizing device, we were able to achieve rotation sensing on a diode-pumped solid-state ring laser. The resulting frequency response curve is shown on Figure 2 (triangle marks). This curve is non-linear, and deviates upwards from the ideal Sagnac line, with no rotation sensitivity (scale factor equals to zero) at null rotation rate.

The important non-linearity and upwards deviation of the frequency response curve of the solid-state ring laser gyro results from mode coupling in the laser cavity. The first source of coupling is backscattering, which is much stronger than in the Helium-Neon case because diffusion comes not only from the cavity mirrors but also from the solid-state gain medium itself. The second source of coupling is the population inversion grating established in the Nd-YAG crystal because of the gain saturation by an optical standing wave.

The trick to reduce the influence of these two coupling sources is to mount the Nd-YAG crystal on a mechanical device creating a vibration movement along the laser longitudinal axis (see Figure 1). Such a vibration movement benefits the solid-state ring laser gyro in two ways. First, it washes out the population inversion grating. For this, the vibration amplitude must be such that each atom is no longer confined into a dark or a bright fringe of the optical standing wave, but rather sees on average the same optical intensity as all others. Furthermore, the vibration frequency must be fast enough for the atoms to be sensitive to the average (rather than instantaneous) optical intensity. In practice, it has to be even faster to avoid parametric resonances between

the vibration frequency and the Sagnac frequency. The second positive effect of crystal vibration on the solid-state ring laser gyro is to Doppler-shift light diffused by the moving gain medium. Thanks to this effect, light from one mode backscattered on the crystal into the counter-propagating mode will be no longer resonant with the latter, resulting in a strong reduction of crystal-induced linear coupling.

The experimental frequency response curve of the solid-state ring laser gyro with crystal vibration at a frequency of about 168 kHz is shown on Figure 2 (circle marks). As can be seen, the non-linearity is strongly reduced in comparison to the non-vibrating case, and the curve has a typical downwards deviation similar to the Helium-Neon ring laser gyro case. This result can be interpreted as follows: since the two previously mentioned couplings (population inversion grating and crystal-induced diffusion) have been suppressed by crystal vibration, we are left only with the coupling resulting from mirror-induced diffusion (scattering), as it is the case of a Helium-Neon ring laser gyro. The size of the lock-in zone that can be deduced from Figure 2 is typically two orders of magnitude bigger than what can be found on a high-performance Helium-Neon ring laser gyro, which we attribute to the quality of our mirrors.

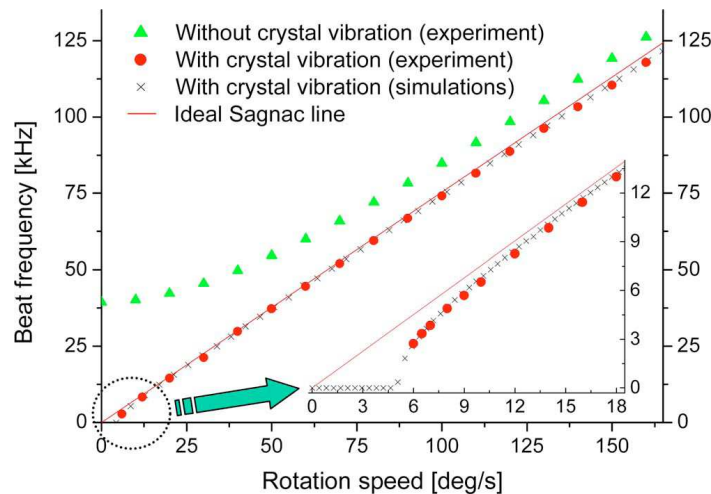


Figure 2. Experimental frequency response curve of our prototype solid-state ring laser gyro with (circle marks) and without (triangle marks) crystal vibration. Also shown (crosses) is the result of numerical simulations in the vibrating crystal case. When the crystal is vibrating, the frequency response curve goes downwards at low rotation rates, similarly to what would be expected for a Helium-Neon ring laser gyro.

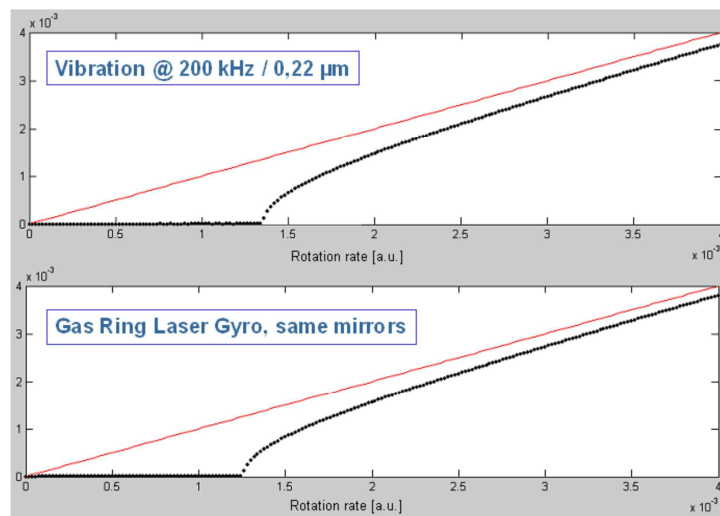


Figure 3. Comparison of the frequency responses of the solid-state ring laser gyro with vibrating crystal (above) and of the Helium-Neon ring laser gyro (below) with identical values of the mirror-induced backscattering coefficient (numerical simulations).

To go further, we have performed numerical simulations of the solid-state ring laser gyroscope with high quality mirrors. Although the solid-state ring laser gyro is very different, in terms of laser dynamics, from the Helium-Neon ring laser gyro, it can be seen on Figure 3 that when the crystal is properly vibrated they have the same dead zone size, determined only by the backscattering coefficient of the non-vibrating scattering part, i.e. the

mirrors. Moreover, we have implemented numerically a statistical study of the angular random walk for the solid-state ring laser gyro with crystal vibration under the usual dithering process that is typically used for Helium-Neon ring laser gyros (including random changes in the dithering amplitude to avoid dynamical lock-in). We have performed the same simulations for the Helium-Neon ring laser gyro with equivalent (high-quality) mirrors. The result (reported on Figure 4) shows no significant difference between the two cases.

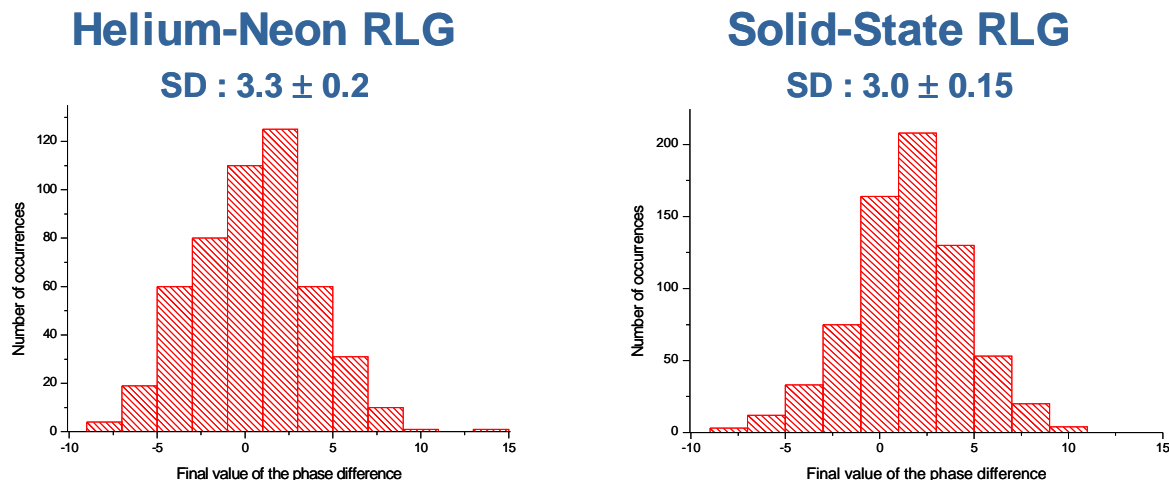


Figure 4. Comparison of the frequency responses of the solid-state ring laser gyro with vibrating crystal (above) and of the Helium-Neon ring laser gyro (below) with identical values of the mirror-induced backscattering coefficient

In conclusion, we expect, considering the results of our numerical simulations, that the solid-state ring laser gyro will have the same behavior as the Helium-Neon ring laser gyro in terms of angular random walk. In both cases, the ultimate limit will be determined by the diffusion rate of the cavity mirrors.

The next developments on our prototype solid-state ring laser gyro include changing the current mirrors for low-diffusion (gyroscope grade) 1064nm mirrors. The latter have been successfully fabricated by LMA Lyon, and are in the process of being assembled on our new device. Another thing being implemented on our prototype is the stabilization of the overall laser intensity, to avoid bias fluctuations due to the residual non-linearity at higher rotation rates. Finally, we are building a numerical control of the differential losses to replace the analogical scheme described in this paper. In particular, it is important to monitor precisely the current flowing inside the solenoid around the gain medium at any time, to compensate for the bias resulting from the (small but nonzero) nonreciprocal rotation of the states of polarization used for creating the differential losses. Suppression of relaxation noise in the Nd-YAG laser is also an important issue, which will be addressed by an additional numerical control of the pump intensity in the 10-30 kHz range.

TOWARDS A RESONANT HOLLOW-CORE FIBER OPTICS GYROSCOPE

The second approach, lower in TRL, is the passive resonant laser gyroscope using a hollow-core fiber cavity. The basic principle of this kind of gyroscope is to probe (using a laser) the eigenfrequencies of two counter-propagating modes of a passive cavity to measure Sagnac effect, a technique that has been early demonstrated in the eighties. The interest for this kind of gyroscope has been recently revived thanks to the advent of narrow-linewidth semiconductor lasers and hollow-core fibers. The latter potentially offer the possibility to build a fiber cavity with reduced non-linear effects (typically two orders of magnitude smaller than for regular fibers), which is a strong asset for optical gyroscopes. It is also potentially more robust to thermal fluctuations, mechanical stress and radiation effects.

In the following, we will assess theoretically the shot-noise sensitivity limit of a resonant gyro based on a realistic hollow-core fiber cavity. The frequency difference Δf between the two counter-propagating modes is:

$$\Delta f = \frac{4A}{\lambda L} \theta,$$

where A is the area enclosed by the cavity and L its perimeter, while λ and θ are the optical wavelength and the rotation rate respectively. As a first remark, we shall note that the scale factor $\frac{4A}{\lambda L}$ is largely independent of the fiber length: if we consider a coil with N_{turn} fiber turns compared with a single loop of equivalent size, the area will be N_{turn} times bigger, and so will be the perimeter. Consequently, the ratio A/L will be unchanged. In the

following, we will thus replace A/L with $D/4$, which is equivalent in the case of a circular configuration with diameter D . For a rotation measurement involving N photons, the minimum measurable rotation rate is thus:

$$\delta\dot{\theta}_{\min} = \frac{\lambda L}{4A} \delta f_{\min} = \frac{\lambda}{D} \frac{\Gamma}{\sqrt{N}},$$

where Γ is the cavity linewidth. The number of photons used for the measurement can be related to the optical power P and the measurement time T by $N = PT/(h\nu)$, hence the following expression for the angular random walk (typically expressed in deg/ $\sqrt{\text{hour}}$):

$$\delta\dot{\theta}_{\min} \sqrt{T} = \frac{\Gamma}{D} \sqrt{\frac{hc\lambda}{P}}. \quad (\text{equation 1})$$

We have built a resonant cavity based on a 50 μm hollow core Kagome fiber from XLIM, following the sketch of figure 5. The resonance peaks of the ring cavity can be observed on figure 6, where the frequency of the laser source is linearly swept.

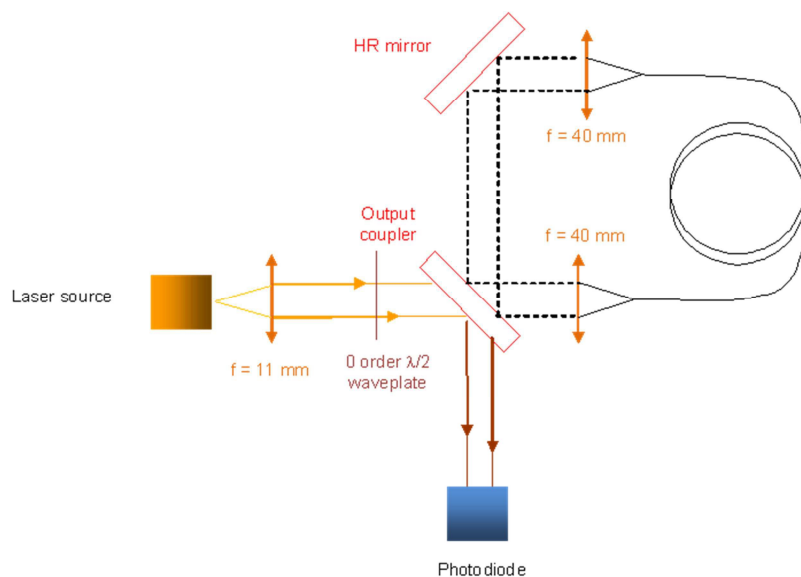


Figure 5: sketch of the resonant cavity and the optical setup used to characterize it. The cavity perimeter is 3.2m, including 3m of hollow core fiber.

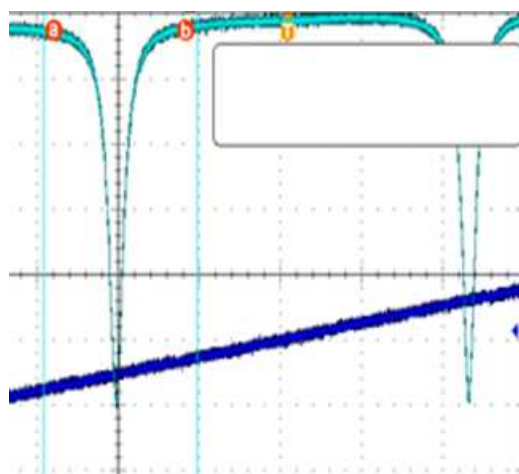


Figure 6: resonance peaks of the hollow core fiber cavity (the dark blue line corresponds to the laser frequency scan). The estimated finesse and contrast are $F \approx 20$ and $C \approx 85\%$ respectively.

The ultimate performance of a resonant gyro based on this hollow core fiber cavity can be assessed from equation 1 and figure 6. On the latter, it can be seen that the finesse (corresponding to the ratio between the distance between two adjacent peaks and the width of one peak) is on the order of 20. Given the fact that the free spectral range (distance between two adjacent peaks) is $c/L \approx 100$ MHz, this leads to the experimental

estimate $\Gamma \approx 5$ MHz. Inserting this value in equation 1 with $D = 15$ cm, $\lambda = 1.5$ μm and $P \approx 1$ mW leads to the following estimate for the shot-noise limit: $\delta\dot{\theta}_{\min}\sqrt{T} \approx 2 \times 10^{-3}$ deg/ $\sqrt{\text{hour}}$, which is already in the high-performance range.

In conclusion, we have performed some preliminary experiment showing that the high performance should be attainable on a resonant hollow core fiber optic gyroscope, provided the latter can be operated in the shot-noise limited regime. With this respect, the recent experiments reported in [1] are very promising, with performance in the 1×10^{-2} deg/ $\sqrt{\text{hour}}$ reported on a resonant fiber optic gyroscope (involving regular optical fiber).

CONCLUSION

We have presented in this paper two novel approaches, which aim to reduce the size and cost of optical gyroscopes while increasing reliability in space environments. Beyond the space domain, these new sensors could make autonomous positioning available to new platforms such as UAVs, and fill the gap between MEMS and high-end optical gyros in the near future.

ACKNOWLEDGEMENT

This work is supported by the European Space Agency under contracts 20856/07/NL/CP and 4000103370/11/NL/Cbi, and by the French National Agency (ANR) in the frame of its "2014 Blanc" programme ("PHOBAG" project).

REFERENCE

- [1] Qiu, T., Wu, J., Strandjord, L. K., & Sanders, G. A, "Performance of resonator fiber optic gyroscope using external-cavity laser stabilization and optical filtering." OFS2014 23rd International Conference on Optical Fiber Sensors. International Society for Optics and Photonics, 2014.